Angewandte
Chemie

Electron Transfer

Study of Anisotropic Interfacial Electron Transfer Across a Semiconductor/Solution Interface by Time-Resolved EPR Spectroscopy**

Kimio Akiyama, Shinji Hashimoto, Sachiko Tojo, Tadaaki Ikoma, Shozo Tero-Kubota, and Tetsuro Majima*

Interfacial electron transfer between molecular adsorbates and semiconductor nanoparticles has been investigated

---

[*] Prof. Dr. K. Akiyama, S. Hashimoto, Dr. T. Ikoma,
Prof. Dr. S. Tero-Kubota
Institute of Multidisciplinary Research for Advanced Materials
Tohoku University
Sendai 980-8577 (Japan)
Fax: (+81) 22-217-5612
E-mail: akiyama@tagen.tohoku.ac.jp
Dr. S. Tojo, Prof. Dr. T. Majima
The Institute of Scientific and Industrial Research (SANKEN)
Osaka University Mihogaoka 8–1
Ibaraki, Osaka 567-0047 (Japan)

[**] This research was supported by a Grant-in-Aid for Scientific Research (No. 15350074) and a Priority Area (417) from the Ministry of Education, Science, Sports, and Culture, Japan. K.A. acknowledges support from CREST (Core Research for Evolutional Science and Technology) of the Japan Science and Technology Agency (JST).

DOI: 10.1002/ange.200461681

intensively in recent years. The elementary reaction can be written as Equation (1):

$$\mathrm{S} + h\nu \rightarrow \mathrm{S}^* \rightarrow \mathrm{S}^+ + \mathrm{e}^-_{\mathrm{surf}}(\mathrm{TiO_2}) \rightarrow \mathrm{S}^+ + \mathrm{e}^-_{\mathrm{CB\ or\ trap}}(\mathrm{TiO_2}) \qquad (1)$$

In this process the dye linked covalently to the TiO_2 through a carboxy group is excited from the ground state S to the excited state S*. The excited dye molecule then acts as an electron donor, and transfers an electron to the surface states and subsequently to the conduction band of colloidal TiO_2. A high quantum efficiency for the conversion of light energy into electricity in dye-sensitized solar cells requires the fast injection of electrons combined with a very slow back transfer of electrons.[1–11] Charge recombination associated with dye-sensitized TiO_2 systems has been rationalized in terms of the inverted Marcus region, where the recombination rate is slowed because of a highly exergonic reaction.[12–14]

The charge-separated state is one of the key intermediates in the photosensitization of electron transfer across the semiconductor/solution interface. The electron in the conduction band reverts to the ground state by recombination, or is trapped on an interior Ti^{3+} ion. The dye molecule remains as the radical cation, which is composed of the charge-separated state and the trapped electron within the TiO_2 particle. Time-resolved EPR (TREPR) spectroscopy has been applied successfully to obtain precise information on transient paramagnetic species. In nanocrystalline TiO_2 particles where bidentate ligands were used as electron donors, polarized EPR spectra originating from a limited distribution of geometries were interpreted by the fixed relative orientation of the magnetic tensor corresponding to the trapped electron and trapped hole.[15] Herein, we report the observation of charge-separated states of TiO_2 nanoparticles sensitized with xanthene dye. We determined the distances between the electron and the dye radical cation as well as their relative orientations by analysis of spin-polarized EPR spectra.

Colloidal TiO_2 particles were prepared by controlled hydrolysis of $TiCl_4$ at 2 °C and further dialysis of the sol.[16] The mean particle size was determined to be about 22 nm by dynamic light scattering studies. The two xanthene dyes (fluorescein (FL) and dichlorofluorescein (FL-Cl_2)) used in the experiments were obtained from Tokyo Kasei and were purified by recrystallization from ethanol before use. The output (coumarin 480, 485 nm) of a dye laser (Lumonics, HD300) pumped by an excimer laser (Lambda Physik COMPex 102) was used for excitation of FL and FL-Cl_2. The detection system for the TREPR signal has been described elsewhere.[17] A helium-flow cryostat (Oxford ESR900) was utilized for measurements at low temperatures.

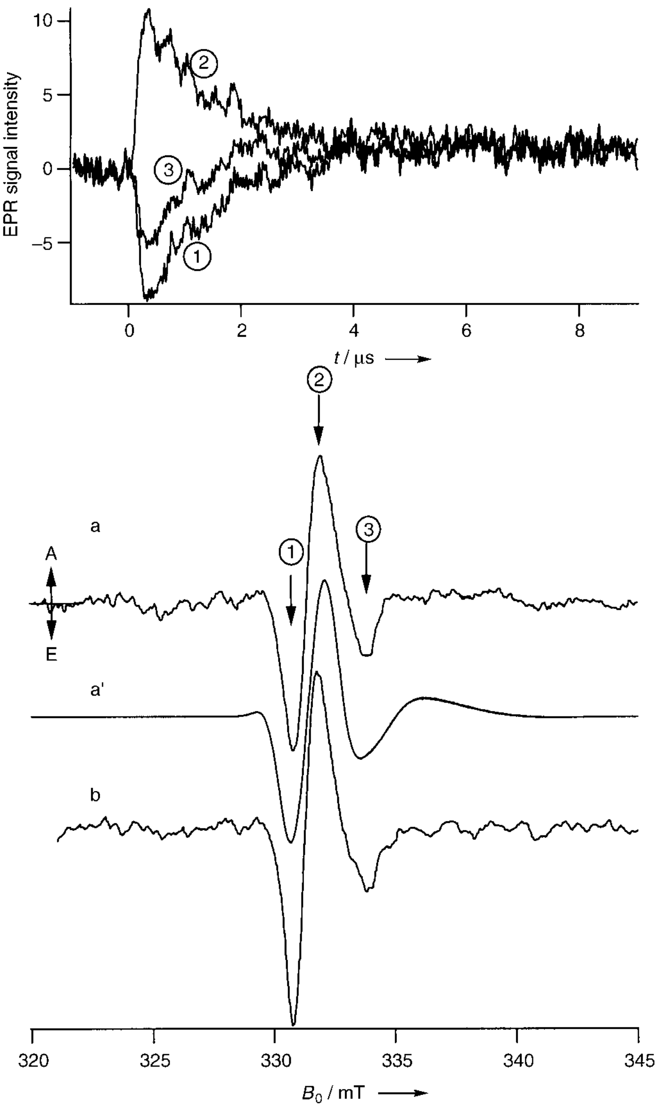

Figure 1. Top: temporal behavior of the polarization at different magnetic fields. Bottom: Time-resolved EPR spectra of FL (a) and FL-Cl_2 (b) adsorbed on colloidal TiO_2 nanoparticles observed at 500 ns after excitation with a laser pulse with a wavelength of 485 nm at 30 K, and the simulated spectrum (a′).

Spin-polarized EPR spectra were observed after excitation with visible light of xanthene dyes adsorbed on colloidal TiO_2 (Figure 1). The polarization patterns (EAE), where A and E denote the enhanced absorption and emission of microwaves, respectively, were essentially identical for the two dye/TiO_2 systems. These results indicate that the precursor state responsible for injection of electrons into the TiO_2 nanoparticle has the same spin multiplicity in the two cases. Since the quantum yields of intersystem crossing in these dyes are very small, electron injection can be expected to occur from the excited singlet precursor state.[18] The polarized signals in each canonical magnetic field decayed with the same rate (approximately $1.0\times10^6\,s^{-1}$), with the phase of the polarization maintaining the EAE pattern during the decay.

The polarized spectra can be readily interpreted in terms of the polarization mechanism of the spin-correlated radical pair (SCRP), where coherent spin singlet/triplet mixing takes place within the radical pair.[19–22] For the calculation we assumed an axial symmetric **g** tensor ($g_\parallel = 1.958$ and $g_\perp = 1.988$) for the trapped electron on TiO_2 and isotropic g values for the dye radical cations.[23] From consideration of the contribution from unresolved hyperfine interactions, an anisotropy of the line widths, $\Delta H_\parallel = 0.8$ and $\Delta H_\perp = 0.3$ mT, was also assumed for the trapped electron. However, isotropic line widths were used for the dye radical cations because of the expected significant delocalization of the unpaired electron. Exchange (J_{SS}) and dipolar (D_{SS}) interactions were the parameters used for simulation of the observed SCRP signals. D_{SS} is given by $D_{SS}\,R^3 = -2.786$ mT nm^3, in which R is the separation of the two unpaired electrons in the molecular center if a point dipole approximation is assumed. According to empirical estimates of the exchange coupling, the value of J_{SS} is negligible compared to the dipolar coupling for distances larger than 1.5 nm.[24–26]

We first calculated the spectrum under the assumption that the dye radical cation is distributed randomly on the surface of TiO_2. However, the observed spectral patterns could not be reproduced satisfactorily. As the local symmetry of the magnetic interactions of a trapped electron on a TiO_2 colloidal nanoparticle is highly anisotropic, the relative orientation between the **g** tensor of the trapped electron and the dipolar tensor of the electron–hole (dye radical cation) pair should be taken into account. In addition, the spin dynamics in the radical pair can also influence the polarization pattern. Unfortunately, the recombination rate of the radical pair at cryogenic temperatures has not been determined. We assumed for the calculation that the recombination rate of the singlet radical pair was of the same order as the polarization decay. The calculated SCRP spectra with different angles ϕ between the **g** tensor of the trapped electron and the dipolar tensor ($\mathbf{Z_d}$) are shown in Figure 2. The EAE polarization patterns were obtained when the angle was set between 90 and 100°. J_{SS} and D_{SS} values corresponding to a distance of 1.6 nm between two unpaired electrons were used for the calculation. The calculated results assuming positive values of J_{SS} are shown in Figure 2. The spectral widths were not significantly affected beyond a radical separation of 1.5 nm, because the small magnetic interaction between two unpaired electrons becomes almost equivalent to the line width. Thus, from the present analysis, we found the separation of the two unpaired electrons was greater than 1.5 nm. Since the size of the dye molecules is known, the trapped electron can be said to be localized at about 0.5 nm from the surface.

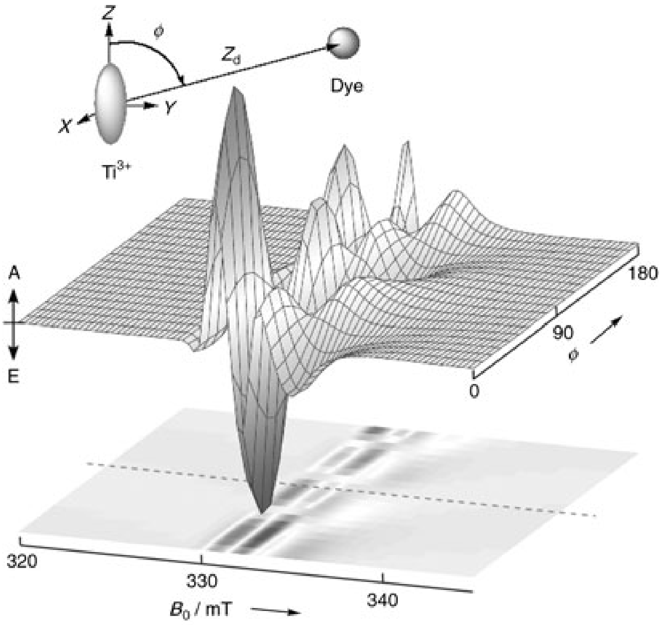

Figure 2. Calculated EPR spectra with different angles between the **g** tensor of the trapped electron and the dipolar tensor of the charge-separated state. The parameters used in the calculation are described in the text.

We obtained the simulated spectra of FL as shown in Figure 1a′ by using the same parameters (J_{SS}, D_{SS}, ϕ, and **g** tensor of the trapped electron). The spectrum observed in the FL-Cl_2/TiO_2 system was also reproduced by using essentially identical parameters. The deviation from the observed spectra can be ascribed to the distribution of dye molecules around ϕ on the TiO_2 colloidal semiconductor. To obtain the best fit of the observed EPR spectra we assumed a positive sign for the exchange interaction. As mentioned above, slow back electron transfer to the dye ground state occurs in the Marcus inverted region where recombination is slowed because of a large change in the free energy of the reaction. The sign of the exchange interaction between the radical pairs is determined by the charge-transfer interaction between the radical ion pair state and the nearby charge-recombined state.[27,28] The locally excited triplet state in the singlet precursor reaction systems effectively perturbs the radical ion pair states because of the small energy difference. The triplet radical ion pair state is selectively stabilized by perturbation from the locally excited triplet state through the electronic coupling, thus leading to positive J values.

The recombination rates for xanthene dye/TiO_2 systems were reported to range from several picoseconds up to microseconds and even milliseconds.[1–11] Colloidal TiO_2 particles had previously been shown to have a crystal structure corresponding to that of anatase.[29] The negatively charged dye molecule reacts with a positively charged Ti-hydroxy group and becomes bound to the Ti atom through formation of a bidentate surface complex. The electron injected from the excited dye molecule recombines through a geminate recombination pathway, but is also trapped in states (assigned to interior Ti^{3+} ions having D_{2d} symmetry) lying below the edge of the conduction band of the TiO_2 nanoparticle. A distribution of energetically different trap sites for the electron and its environments could be responsible for such recombination kinetics. The polarized EPR spectrum is observed at timescales of the order of a microsecond or shorter. In the analysis of the SCRP signal of the xanthene dye/TiO_2 system the relative orientations of the **g** tensor of the trapped electron and the vector of the dipole–dipole interaction between two unpaired electrons are fixed regardless of the expected uniform adsorption of the dye molecules on the surface of the TiO_2 nanoparticle. The observed polarized spectra were well-reproduced at an angle of around 90° between the **g** tensor of the electron and the dipolar tensor. This finding indicates that electron transfer across the semiconductor surface occurs with high orientational selectivity with respect to the radical stabilized on the xanthene dyes. As a result, an anisotropic orientation between the trapped electron and the hole is realized in the microsecond-scale interval after the injection of electrons. The relative orientation of trapped electrons versus cationic dyes as reported here may correspond to a residual distribution that remains after most of the recombination events have already occurred on a much shorter time scale (femtoseconds to picoseconds) than corresponds to the time resolution of the present experiment.

In conclusion, we have observed polarized EPR spectra of xanthene dyes adsorbed on colloidal TiO_2 at low temperatures upon excitation with pulses of visible light. The SCRP polarization mechanism was adopted to analyze the polarization patterns and line shapes in detail. The positive sign of the exchange interaction of the radical pair was ascribed to charge recombination in the Marcus inverted region. The relative orientation of the magnetic tensor of the trapped electron and the dye radical cation is fixed, thus leading to orientational selectivity in electron transfer across the semiconductor nanoparticle.

Received: August 17, 2004
Revised: March 12, 2005

Keywords: electron transfer · EPR spectroscopy · nanoparticles · radical pair · semiconductors

---

[1] J. E. Moser, M. Grätzel, *J. Am. Chem. Soc.* **1984**, *106*, 6557–6564.

[2] J. E. Moser, M. Grätzel, *Chem. Phys.* **1993**, *176*, 493–500.

[3] *Surface Electron Transfer Process* (Eds.: R. D. Miller, G. L. McLendon, A. J. Nozik, W. Schmikler, F. Willig), VCH, New York, **1995**.

[4] S. Yan, J. T. Hupp, *J. Phys. Chem.* **1996**, *100*, 6867–6870.

[5] Y. Tachibana, J. E. Moser, M. Grätzel, D. R. Klug, J. R. Durrant, *J. Phys. Chem.* **1996**, *100*, 20056–20062.

[6] R. Argazzi, C. A. Bignozzi, T. A. Heimer, F. N. Castellano, G. J. Meyer, *J. Phys. Chem. B* **1997**, *101*, 2591–2597.

[7] D. Liu, R. W. Fessenden, G. L. Hug, P. V. Kamat, *J. Phys. Chem. B* **1997**, *101*, 2583–2590.

[8] T. Hannappel, B. Burfeindt, W. Storck, F. Willig, *J. Phys. Chem. B* **1997**, *101*, 6799–6802.

[9] M. Hilgendorff, V. Sundström, *J. Phys. Chem. B* **1998**, *102*, 10505–10514.

[10] S. Cherian, C. C. Wamser, *J. Phys. Chem. B* **2000**, *104*, 3624–3629.

[11] I. Martini, J. H. Hodak, G. V. Hartland, *J. Phys. Chem. B* **1998**, *102*, 607–614.

[12] H. Liu, J. N. Preiskorn, J. T. Hupp, *J. Am. Chem. Soc.* **1993**, *115*, 4927–4928.

[13] I. Martini, J. H. Hodak, G. V. Hartland, *J. Phys. Chem. B* **1998**, *102*, 9508–9517.

[14] X. Dang, J. T. Hupp, *J. Am. Chem. Soc.* **1999**, *121*, 8399–8400.

[15] A. A. Dubinski, G. D. Perekhodtsev, O. G. Poluektov, T. Rajh, M. C. Thurnauer, *J. Phys. Chem. B* **2002**, *106*, 938–944.

[16] S. Tojo, T. Tachikawa, M. Fujitsuka, T. Majima, *Chem. Phys. Lett.* **2004**, *384*, 312–316.

[17] Y. Kamata, K. Akiyama, S. Tero-Kubota *J. Phys. Chem. A* **1999**, *103*, 1714–1718.

[18] A. W.-H. Mau, O. Johansen, W. H. F. Sasse, *Photochem. Photobiol.* **1985**, *30*, 81.

[19] G. L. Closs, M. D. E. Forbes, J. R. Norris, *J. Phys. Chem.* **1987**, *91*, 3592–3599.

[20] P. J. Hore, D. A. Hunter, C. D. McKie, A. J. Hoff, *Chem. Phys. Lett.* **1987**, *137*, 495–500.

[21] P. J. Hore in *Advanced EPR in Biology and Biochemistry* (Ed.: A. J. Hoff), Elsevier, Amsterdam, **1989**.

[22] D. Stehlik, C. H. Bock, J. Petersenn, *J. Phys. Chem.* **1989**, *93*, 1612–1619.

[23] T. Rajh, J. M. Nedeljkovic, L. X. Chen, O. Poluektov, M. C. Thurnauer, *J. Phys. Chem. B* **1999**, *103*, 3515–3519.

[24] R. E. Coffmann, G. B. Buettner, *J. Phys. Chem.* **1979**, *83*, 2387–2392.

[25] M. D. E. Forbes, G. L. Closs, P. Calle, P. Gautam, *J. Phys. Chem.* **1993**, *97*, 3384–3389.

[26] G.-H. Goudsmit, H. Paul, A. I. Shushin, *J. Phys. Chem.* **1993**, *97*, 13243–13249.

[27] S. Sekiguchi, Y. Kobori, K. Akiyama, S. Tero-Kubota, *J. Am. Chem. Soc.* **1998**, *120*, 1325–1326.

[28] Y. Kobori, K. Akiyama, S. Tero-Kubota, *J. Chem. Phys.* **2000**, *113*, 465–468.

[29] C. Kormann, D. W. Bahnemann, M. R. Hoffmann, *J. Phys. Chem.* **1988**, *92*, 5196–5201.